We are IntechOpen,
the world's leading publisher of
Open Access books
Built by scientists, for scientists

6,900
Open access books available

186,000
International authors and editors

200M
Downloads

Our authors are among the

154
Countries delivered to

TOP 1%
most cited scientists

12.2%
Contributors from top 500 universities

CLARIVATE ANALYTICS
BOOK CITATION INDEX
INDEXED

WEB OF SCIENCE™

Selection of our books indexed in the Book Citation Index
in Web of Science™ Core Collection (BKCI)

Interested in publishing with us?
Contact book.department@intechopen.com

Numbers displayed above are based on latest data collected.
For more information visit www.intechopen.com

Ecologically Friendly Polymer-Metal and Polymer-Metal Oxide Nanocomposites for Complex Water Treatment

Amanda Alonso, Julio Bastos-Arrieta,
Gemma.L. Davies, Yurii.K. Gun'ko, Núria Vigués,
Xavier Muñoz-Berbel, Jorge Macanás, Jordi Mas,
Maria Muñoz and Dmitri N. Muraviev

Additional information is available at the end of the chapter

1. Introduction

The physical characteristics of nanomaterials, those with a size smaller than 100 nm, are known to be substantially dependent on their size scale. The increase of interest in nanotechnology studies has been due to the incorporation of nanoparticles (NPs) into commercial available products.

Thus, the development of methods for the synthesis of NPs with a narrow size distribution, the techniques of separation and preparation of customized of engineered nanoparticles is one of the most important points of research to focus in.

By taking into account some parameters during NPs preparation, such as: time, temperature, stirring velocity and concentrations of reactants and stabilizing reagents, one can obtain the ideal distribution and morphology of these novel materials [1].

In this regard,polymeric supports play a very important role for several reasons including, the ease of their preparation in the most appropriate physical forms (e.g., granulated, fibrous, membranes, etc.), the possibility to produce the macroporous matrices with highly developed surface area and some others. However, the immobilization of NPs on the appropriate polymeric support represents a separate task [2] and thus, the incorporation of poly-

mers as support for NPs synthesis is another way to control the growth of NPs as well as preventing the NPs aggregation and their release.

Embedded NPs in polymer matrix have gained interest in the past years, because of the unique applications of the final nanocomposite materials, for example, optical, magnetic, sensors and biosensors [3–11].

Several parameters of the polymeric matrices may be considered for their use on the synthesis of nanocomposites as it is discussed in the following sections.

1.1. Ion Exchange Polymers

One simple consideration of the ion exchange process is the equivalent exchange of ions between two or more ionized species located in different phases, at least one of which is an ion exchanger. The process takes place without the formation of chemical bonds by certain equilibrium between charges of ions and, in the case of polymers, functional groups.

Depending on the functional group charge, ion exchangers are called cation exchangers if they bear negative charged functional groups and carry exchangeable cations. Anion exchangers carry anions due to the positive charge of their fixed groups. Chemical interactions could be different for different polymeric and inorganic ion exchanges. However, most of the thermodynamic and kinetic approaches, as well as the practical methods and technologies are essentially the same [12]. Table 1 shows the most common physical and chemical parameters specific for polymeric ion exchangers.

Physical properties	Chemical Properties
Physical structure and morphology	Cross Linking degree
Surface Area	Ionic form(functional groups)
Particle Size	Ion Exchange Capacity(IEC)
Partial Volume in swollen state	Type of matrix

Table 1. General Properties of Ion Exchange Materials [13].

Probably, the first extensive investments in the development of ion exchangers and ion exchange processes were done bearing in mind the potential application for isotope separation in nuclear industry, although nowadays one of the most common applications of these materials is in water purification processes among other applications of interest as is shown in Table 2.

Functional groups define chemical properties, by bearing on surface a negative or positive charge. Due to this fact, different dissociation properties of groups leads to a difference among strong and weak exchangers; which are recognized similar to that of strong and weak electrolytes. Table 3 shows some of the most common types of cation and anion exchangers.

Application	Brief Description
Water Treatment	Preparation of pure and ultrapure deionized water
	Potable Water preparation
	Water Softening
Food Industry	Removing off tasters and odors.
	Deacidification of fruit juice
	Recovery of glutamic acid
Nuclear Industry	Separation of uranium isotopes
	Final storage of radioactive waste.
	Waste decontamination
Pulp and Paper Industry	Removal of inorganic salts from liquors
	Detoxification of by-products transferred to bio-cultivation

Table 2. Different applications of ion exchange materials [12,13].

Cation Exchange groups (Negatively charged)	Anion Exchange Groups (Positively Charged)
Sulphonic SO_3^-	Quaternary Amonium $-(N\text{-}R_3)^+$
Carboxilic: COO^-	Phosphonium: $-(P\text{-}R_4)^+$
Arsenate: AsO_3^-	Sulphonium: $-(S\text{-}R_3)^+$
Phosphate $-PO_3^{2-}$	

Table 3. Functional Groups in Ion Exchange Polymers [13].

Ion exchange capacity (IEC) is the main feature of ion exchange materials. An ion exchanger can be considered as a "reservoir" containing exchangeable counterions. The counterion content, in a given amount of material, is defined essentially by the amount of fixed charges which must be compensated by the counterions and thus, is essentially constant [6,7].

Some facts must be considered to define IEC: availability of functional groups for exchange re-action, the macrostructure architecture, swelling degree and the size of the ions to be exchanged.

Depending on the final application of an ion exchange polymer (e.g., granulated resins), a pre-treatment stage is advised in order to obtain an enhanced and optimal exchange capaci-ty. For cationexchanger resins an acid stage pretreatment (usually HCl 0.1 M) is the more advisable, as for the anionexchangerresin would be a basic stage pre-treatment (usually NaOH 0.1 M).

Regarding the applications of the ion exchange resins, they have been used in pharmaceu-tics and food industry which is determined by another advantage of these materials: while

being chemically active, they are highly stable in both physical and chemical senses and, as a result, do not contaminatethe final product.

Concretely, the use of the functional ion exchange polymers as supports for the synthesis of metal nanoparticles (MNPs) and metal oxide nanoparticles (MONPs) [14] has in this sense, one most important advantage dealing with the possibility to synthesize the NPs of interest directly at the "point of use", i.e. on the supporting polymer by an "in-situ" reaction. For instance, in the case of the metal catalyst nanoparticles, this results in the formation of cata‐lytically-active polymer-metal nanocomposites [6,7,15].

Overall, this chapter focuses on the feasible application of ion exchange polymeric matrices (i.e., both cation and anion granulated exchangers resins) used as support for MNPs and MONPs synthesized by using the developed Intermatrix Synthesis (IMS) methodology [5]-[8,10, 14,16]. This methodology has been shown by the enhancement of the accessibility of the nanomaterial for de desirable final functionality due to the final NPs distribution. The overall combination of certain features of these matrices: cross linking degree, the different solubility in organic solvents, their stability and insolubility in water, etc. offer a wide range of possible applications and functionalities, depending on the embedded NPs nature as well of the type of polymer for a specific final use. For instance, examples of water treatment and catalysis have been presented on several publications of the authors [14,6].Concretely, this chapter is based on the use of these materials for the bacteria elimination on water treatment applications.

2. Intermatrix synthesis of metal nanoparticles

The IMS method represents one of the most efficient and simple techniques for the "in-situ" preparation of metal-polymer nanocomposites. The general principles of IMS apply to all types of polymer matrices and NPs.In general:

- Polymer molecules serve as nanoreactors and provide a confined medium for the synthe‐sis (thus controlling particle size and distribution).

- Polymer molecules stabilize and isolate the generated NPs, thus preventing their aggregation.

In the case of ion exchange matrices, the functional groups that can immobilize metal ions and metal ion complexes are the key points for IMS because they are homogeneously dis‐tributed in the ion exchange matrix and behave as combinations of single isolated nanoreac‐tors generating homogeneous nanocomposites.

The major part of our work in this field has been done with the polymers bearing negative charged functional groups (i.e., cation exchanger polymers containing both carboxylated and sulfonated [5,8,10] functional groups), which first have to be loaded with the desired metal ions (MNP precursors) followed by their chemical reduction to zero-valent state (MNPs) by using an appropriate reducing agent. Several recent publications by the authors describe the IMS of MNPs with the most favorable distribution near the surface of nanocom‐posite for instance for catalytic applications or for killing bacteria by a contact mecha-

nism.This distribution is due to the coupling of the classical IMS methodology with the Donnan Exclusion effect (DEE) [6,7,9,16].

The polymeric matrix bears a charge due to the presence of well-dissociated functional groups. This means that a reducing agent negatively charged (e.g., brohydride BH_4^-) presents the same charge than the support, therefore they cannot penetrate inside the polymer because of the action of electrostatic repulsion. This is known as Donnan Exclusion Effect. It refers to the impossibility to penetrate deeply in a matrix when there is a coincidence between the charge of the outside ions (e.g. from the reducing agent) and the ones of the functional groups on the polymer surface. Thus, an equilibrium between ion concentration (either functional groups or from metal or reducing agent solution) and electrostatic repulsion takes place (Figure 1).
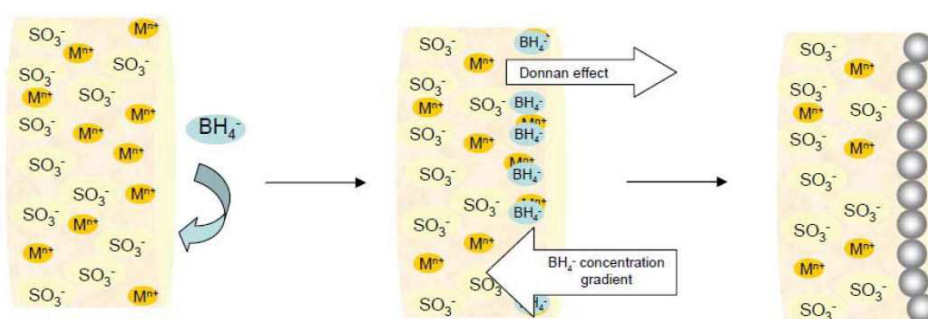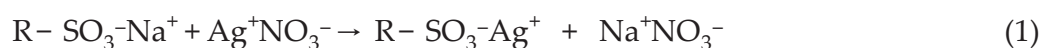

Figure 1. Scheme of IMS on a sulfonated exchange polymer with Donnan Exclusion Effect to obtain MNPs mainly on the polymer surface.

2.1. Traditional and novel versions of IMS technique

The difference between the traditional and the novel version of the IMS technique developed in this study become clear after comparison of the respective reaction schemes, which can be written for the case of formation of Ag-NPs in (a) strong acidic polymers (e.g. containing sulfonated $-SO_3^-$ functional groups)and; (b) strong basic polymers (e.g. containing quaternary ammonium $-NR_4^+$ functional groups)as follows [6,7]:

a) IMS in cation exchanger polymers (traditional version):

1) Metal-loading stage

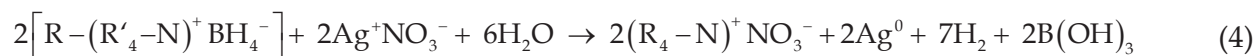$$R- SO_3^-Na^+ + Ag^+NO_3^- \rightarrow R- SO_3^-Ag^+ \ + \ Na^+NO_3^- \tag{1}$$

2) Metal-reduction stage

$$2R-SO_3^-Ag^+ + 2\,NaBH_4 + 6H_2O \rightarrow 2R- SO_3-Na^+ + 2Ag^0 + 7H_2 + 2B(OH)_3 \tag{2}$$

b) IMS in anion exchange polymers (novel version):

1) Reduce-loading stage

$$R-(R'_4-N)^+Cl^- + NaBH_4 \rightarrow (R_4-N)^+BH_4^- + NaCl \tag{3}$$

2) Metal-loading-reduction stage

$$2\left[R-(R'_4-N)^+BH_4^-\right] + 2Ag^+NO_3^- + 6H_2O \rightarrow 2(R_4-N)^+NO_3^- + 2Ag^0 + 7H_2 + 2B(OH)_3 \tag{4}$$

As it is seen from the above reactions, the main difference between (a) and (b) versions of IMS consists in the first stage of the process. In the first case, the functional groups of the polymer are loaded with the desired metal ions, while in the second case, the loading is carried out with the desired reducing ions. The second stage, in the first case, consists on the reduction of metal ions with ionic reducing agent, located in the external solution. As far as the charge sign of reducer anions coincide with that of the polymer matrix, they cannot deeply penetrate inside the polymer due to the action of the DEE and as the result, the reduction process appears to be "localized" near the surface of the polymer.

As the result, the second stage of this version permits to couple the metal-loading and the metal-reduction processes in one step. The metal loading is carried out by using external solution containing metal ions bearing the charge of the same sigh as that of the functional groups of the polymer, what does not allow them to deeply diffuse inside the polymer matrix (due to DEE process). Again, the reduction of metal ions and therefore, the formation of MNPs have to proceed near the surface of the polymer. For obvious reasons the second version of IMS technique (version b) can be classified as a sort of the symmetrical reflection of version (a) as it is shown in Figure 2.
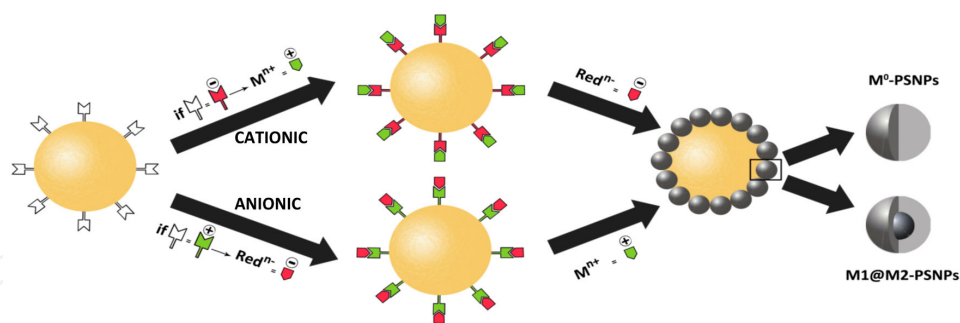

Figure 2. Scheme of IMS steps for the synthesis of NPs by using either a cation or anion granulated exchanger polymer as a matrix, throwing to symmetrical version of IMS influenced by DEE.

In both versions of IMS methodologies shown, DEE plays a very important role as it appears to be responsible for the desired nonhomogeneous distribution of MNPs inside the polymeric nanocomposite. The action of this effect is observed in both cases within the second stage of IMS process (see equations 2 and 4). The following two "driving forces" acting in the opposite directions are responsible for the DEE: 1) the electric field determined by the charge of the polymer matrix and 2) the concentration of the ionic component in the external solution [17,18].

The first force rejects the ions of the same charge as that of the functional groups of the polymer while the second one drives these ions to move into the polymeric matrix. The first force can be hardly varied as it has a constant value determined by the ion exchange capacity of the polymer and the degree of dissociation of its functional groups. The second force can be easily varied by changing the concentration of respective component in the external solution, what has to result in the changes in the composition of the final nanocomposite (MNPs content).

The possibility to use the second approach follows from the above reaction schemes (see reactions 2 and 4). Indeed, after finishing the metal reduction (IMS version a) or the metal-loading-reduction stages (IMS version b) the functional groups of the polymer appear to be converted back into the initial ionic form (Na-form in the first and Cl-form in the second case). This means that in both cases IMS reactions of MNP can be repeated without any additional pretreatment of the ion exchanger. This has to result in the accumulation of a higher amount of the metal (or MNPs) inside the polymer when the same metal precursor is used or, what is more relevant in this work, the possibility of the formation of core-shell NPs (e.g. Ag@Co-NPs, what means a Co-core coated by a Ag-shell). This approach leads to a wide range of possibilities for the applications of core-shell MNPs or MONPs [6,7,10,16,19–22]. Thus, the following Figure 3 shows the range of types of MNPs and MONPs (either monometallic or core-shell bimetallic structures) synthesized by the mentioned methodology presenting different properties for the applications of interest.
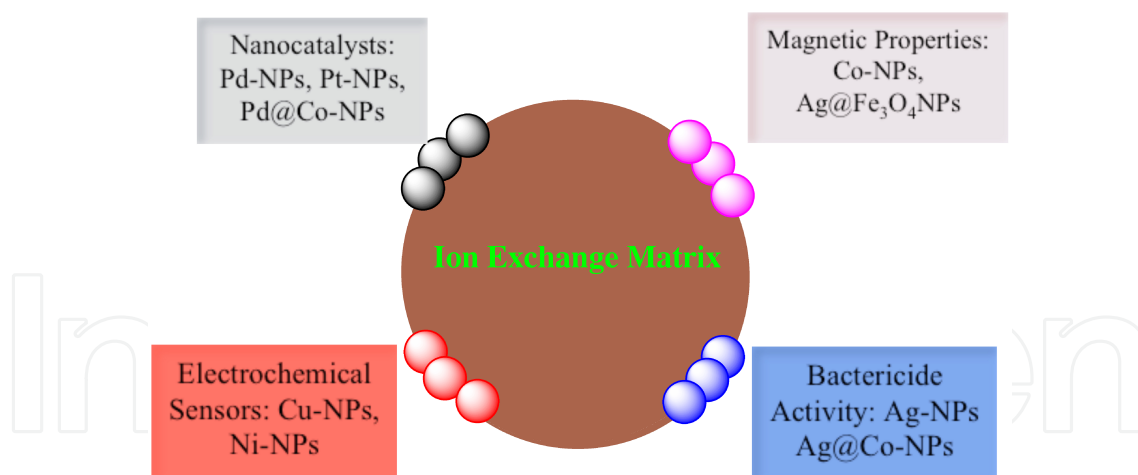

Figure 3. Scheme of IMS feasibility to produce different MNPs or MONPs with an accessible distribution of NPs on polymer surface for different final applications.
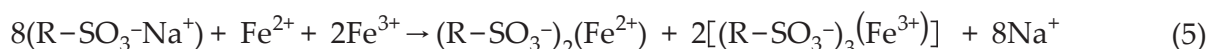
Among all the MNPs and MONPs possibilities, in this chapter, we focused on the synthesis and characterization (Section 3) of monocomponent NPs based on magnetite (Fe_3O_4), cobalt (Co) and silver (Ag) as well as bicomponent core-shell NPs based on $Ag@Fe_3O_4$ and Ag@Co. In these cases, the core is always composed of a magnetic element for its interest regarding the final application and the prevention of MNPs leaching, as it will be discussed in Section 4.

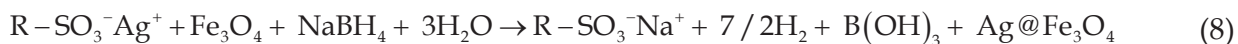# 3. Characterization of nanocomposite materials

In order to understand the enhancement of the properties of the polymeric nanocomposites obtained by IMS technique, a proper material characterization is mandatory and it is presented in this section. The application of these novel materials is presented in later on, and deals with their bactericidal activity for water treatment application.

3.1. Synthesis and sharacterization of sulfonated granulated nanocomposites containing Fe₃O₄- and Ag@Fe₃O₄-NPs

Fe₃O₄ and Ag@Fe₃O₄ nanocomposites were developed by an extension of IMS technique by the coupling of the general precipitation technique of Fe₃O₄-NPs(23)with the IMS methodology as shown in the following reactions:

$$8(R-SO_3^-Na^+) + Fe^{2+} + 2Fe^{3+} \rightarrow (R-SO_3^-)_2(Fe^{2+}) + 2[(R-SO_3^-)_3(Fe^{3+})] + 8Na^+ \qquad (5)$$

$$(R-SO_3^-)_2(Fe^{2+}) + 2[(R-SO^{3-})_3(Fe^{3+})] + 8NaOH \rightarrow 8(R-SO_3^-Na^+) + Fe_3O_4 + 4H_2O \qquad (6)$$

The synthesis of Ag@Fe₃O₄-NPs was performed by the subsequent reduction reaction of Ag⁺ onto Fe₃O₄-NPs surface and within the matrix as follows:

$$R-SO_3^-Na^+ + Fe_3O_4 + Ag^+ \rightarrow R-SO_3^-Ag^+ + Na^+ + Fe_3O_4 \qquad (7)$$

$$R-SO_3^-Ag^+ + Fe_3O_4 + NaBH_4 + 3H_2O \rightarrow R-SO_3^-Na^+ + 7/2H_2 + B(OH)_3 + Ag@Fe_3O_4 \qquad (8)$$

The main characterization techniques for nanomaterials have been used in these systems.

3.1.1. X-Ray Diffraction, XRD

XRD technique was used to determine the crystalline structure of the particles. Figure 4 shows the XRD graphs of Fe₃O₄-NPs as a reference (synthesized by liquid phase method [24] and the sample corresponding to Fe₃O₄-NPs stabilized in a sulfonated polymeric matrix represented as C100E code (from Purolite S.A).

The position and relative intensity of all diffraction peaks from the Fe₃O₄-nanocomposite sample are in good agreement with those for the Fe₃O₄ powder. The relative intensity is lower for the nanocomposite sample due to the "diluting" polymer effect.

3.3.2. Microscopy characterization

The microscopy techniques (e.g., Scanning Electron Microscopy, SEM, and Transmission Electron Microscopy, TEM) allow the characterization of both surface and inside area of the nanocomposites. For instance, the NPs metal concentration profiles, along the cross-sec-

tioned polymeric beads Figure 5), was examined by using SEM technique coupled with En-ergy Dispersive Spectroscopy (EDS). EDS analysis demonstrated that Ag and Fe elements were mostly found on the edge of the bead.In general, this non-homogeneous distribution of the NPs may be attributed to the Donnan Exclusion Effect as shown before for NPs in most of the polymers.
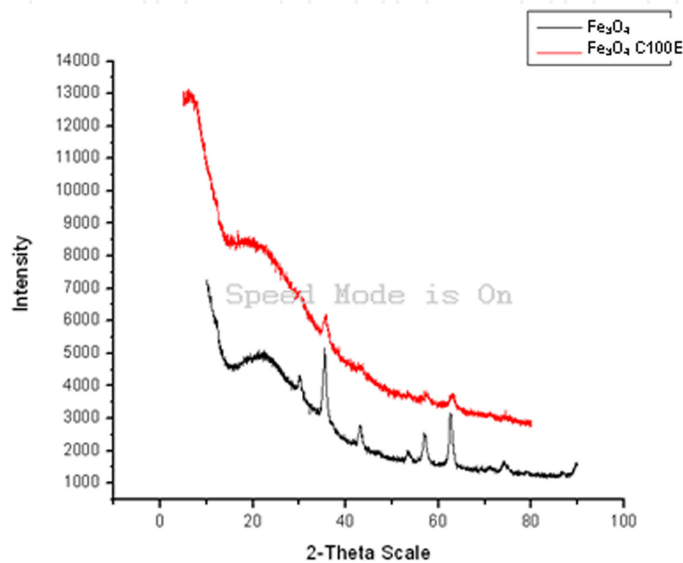

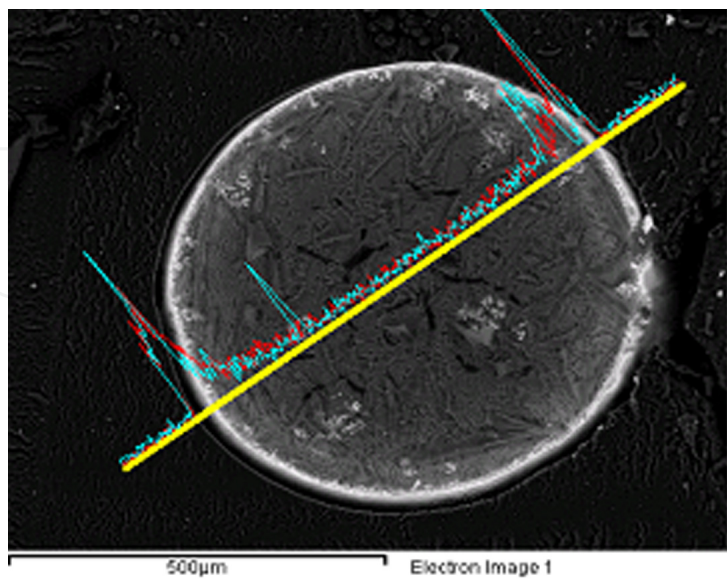**Figure 4.** X-ray diffraction patterns of Fe_3O_4-NPs (black) and, Fe_3O_4-NPs stabilized on sulfonated polymer (red).

Figure 5. SEM image of a cross-sectioned Ag@Fe_3O_4-sulfonated nanocomposites resin and EDS metal content distri-bution profile (Ag in blue line and, Fe in red line).

3.1.3.Thermogravimetric Analysis, TGA

TGA technique is used to determine polymer degradation temperatures in polymer or composite materials [24]. Figure 6 shows the TGA curves for Fe_3O_4- and $Ag@Fe_3O_4$-NPs stabilized in sulfonated resin as well as the corresponding raw polymer.

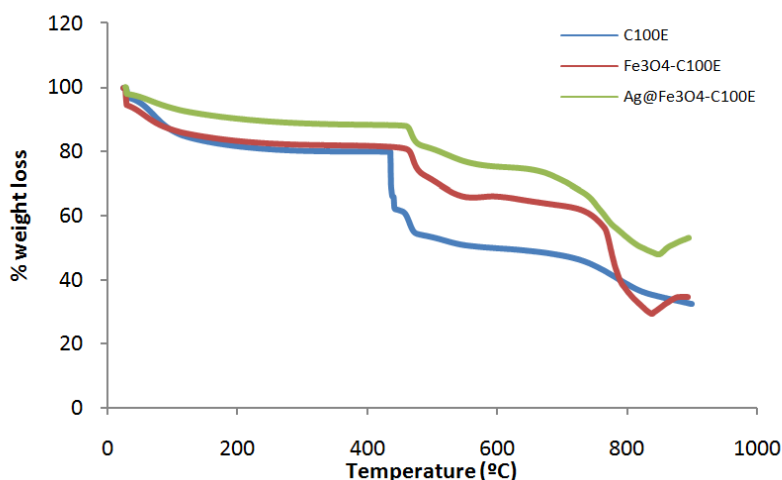**Figure 6.** TGA curves of %weight loss vs temperature of sulfonated samplesFe_3O_4- and $Ag@Fe_3O_4$.

As seen in Figure 6, TGA curves for all samples are characterized by four weight-loss regions, which can be described as follows:

1. The weight loss between 30 and 400ºC can be mainly attributed to adsorbed water molecules, both "free" and strongly "bound" to surface groups from the polymer and the nanoparticles, where applicable.

2. A significant weight loss at 450ºC for all samples. This loss is particularly important for the raw polymer (NPs-free) in comparison with the NPs-modified polymers and can be associated with the loss of the functional groups including free sulfonic functionalities.

3. A third gradual weight-loss is observed between 500ºC and 700ºC and may be attributed to the degradation of the polymer side chains. Again, this loss is less important for the nanocomposite samples.

4. Finally, the weight changes at temperatures higher than 700ºC may be caused by further thermodegradation of the polymer, but is noteworthy that for $Ag@Fe_3O_4$-C100E and Fe_3O_4-C100E nanocomposites, there is weight gain, probably due to the oxidation of the magnetic material from Fe_3O_4 to Fe_2O_3.

As can be seen, lines are almost parallel and only Fe_3O_4-C100E sample shows a quite different behaviour close to 800ºC [24].

3.1.4. Magnetic characterization

As mentioned, the bicomponent core-shell NPs are based on a magnetic core which lead to obtain magnetic properties to the nanocomposite. The characterization of the magnetic properties of the nanocomposites was preceded by using a vibrating sample magnetometer (VSM), as shown in Figure 7 by the representation of the magnetization curves of the samples when a magnetic field is applied. Also, the magnetic behavior of Fe_3O_4-NPs as powder structure (without polymeric support) was analysed.
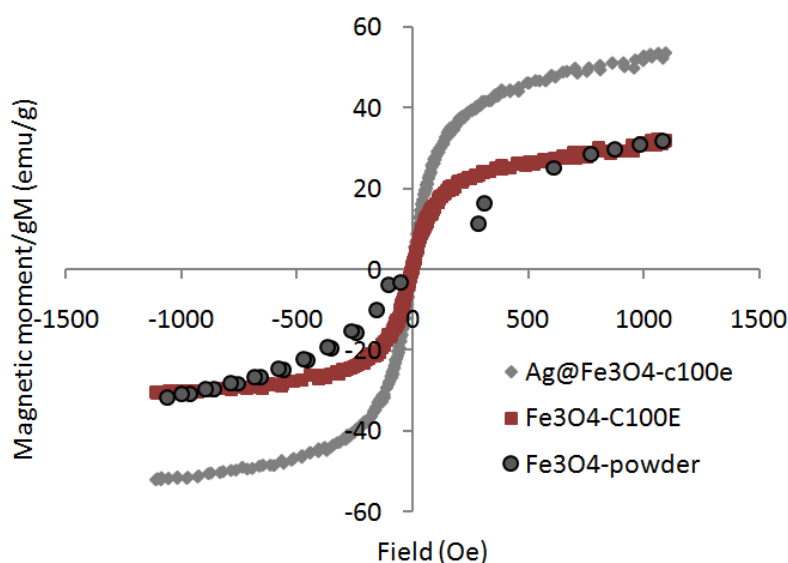

Figure 7. Magnetization curves for Fe_3O_4- and Ag@Fe_3O_4-NPs in sulfonated polymer and for powered Fe_3O_4-NPs.

As shown, superparamagnetic behaviour was observed in all the Fe_3O_4-based nanocomposites and powder. When comparing the magnetization values of the Fe_3O_4-nanocomposite with powdered Fe_3O_4-NPs, similar magnetization values were obtained at aprox. 30 emu/g. Besides, Ag@Fe_3O_4-nanocomposites showed higher magnetic saturation than for those Fe_3O_4 ones. [22–25] This result, as an example, shows the advantage of the nanocomposites containing Ag@Fe_3O_4-NPs since they show the combination of the properties from both components: bactericidal activity from Ag as well as magnetic properties from Fe_3O_4 core.

3.2. Amine-based granulated nanocomposites containing Fe_3O_4- and Ag@Fe_3O_4-NPs(14)

On the other hand, and with the goal of expanding the IMS technique applications, Fe_3O_4- and Ag@Fe_3O_4-NPs were also synthesized in anion exchanger polymers. The granulated resin (in this case, A520E from Purolite), containing quaternary ammonium functional groups ($-NR_3{}^+$), was used as polymeric matrix.
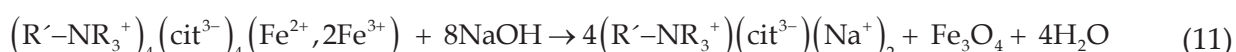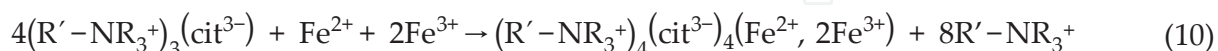
As already introduced, the synthesis of MNPs in anionic exchanger polymers is the "mirror image" methodof the traditional IMS (see Figure 2 and Eqs 3-4). Thus, for the case of the combination of the precipitation technique with the IMS for the synthesis of Fe_3O_4-NPs in

quaternary ammonium based polymers, the use of an initial positively charged element is needed to modify the charge of the raw polymer and lead to the procedure of the synthesis.

The following equations show this synthetic procedure. Initially, the raw material was pre-treated with 1.0 M trisodium citrate, $((CH_2)_2COH)(COONa)_3$, to compensate the positive charge of the polymer (where cit = citrate).

$$3(R'-NR_3^+)(Cl^-) + (Na^+)_3(cit^{3-}) \rightarrow (R'-NR_3^+)_3(cit^{3-}) + 3NaCl \tag{9}$$

Afterwards, the polymer was used for the Fe_3O_4-NPssynthesis :

$$4(R'-NR_3^+)_3(cit^{3-}) + Fe^{2+} + 2Fe^{3+} \rightarrow (R'-NR_3^+)_4(cit^{3-})_4(Fe^{2+}, 2Fe^{3+}) + 8R'-NR_3^+ \tag{10}$$

$$(R'-NR_3^+)_4(cit^{3-})_4(Fe^{2+}, 2Fe^{3+}) + 8NaOH \rightarrow 4(R'-NR_3^+)(cit^{3-})(Na^+)_2 + Fe_3O_4 + 4H_2O \tag{11}$$

Ag@Fe_3O_4-NPs were obtained after the loading with $NaBH_4$ followed by the use of $AgNO_3$.
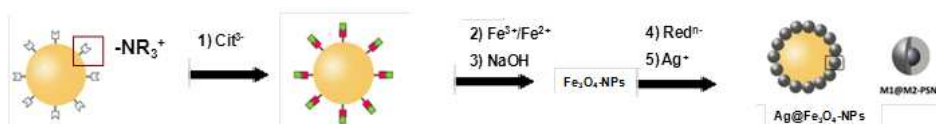
Schematically, Figure 8 describes the synthetic procedure.

Figure 8. Synthetic methodologies for the synthesis of monocomponent Ag-NPs or Fe_3O_4-NPs and bicomponent Ag@Fe_3O_4-NPs stabilized in A520E support

Next, the microscopy characterization and the evaluation of the magnetic properties of these materials are shown.

3.2.1. Microscopy characterization

As described before, SEM technique was used to evaluate the NPs distribution. Thus, Figure 9a shows the metal profile of Ag@Fe_3O_4-NPs stabilized on an anionexchanger polymer. By EDS ScanLine is observed that Ag and Fe co-localize in Ag@Fe_3O_4-nanocomposite matrix. In addition, the particles structure in the nanocomposite was analysed by TEM. Figure 9bshows a magnified TEM image of the edge of the cross sectioned area from Figure 9a with a dispersed distribution of the NPs. By these results, the wide range of systems that can be studied based on IMS technique and the success on their formation is clearly shown.

3.2.3. Magnetic characterization

The magnetic properties of Ag@Fe_3O_4-nanocomposites were determined with a Superconducting Quantum Interference Device (SQUID) and compared with those obtained by polymeric structures only containing Fe_3O_4-NPs.
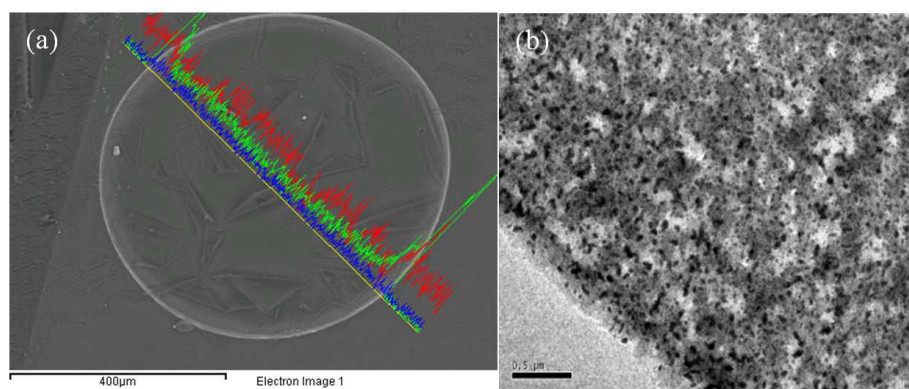
Figure 9. a)SEM images of cross sectioned Ag@Fe$_3$O$_4$-nanocomposite(on A520E matrix).EDS LineScan shows Ag (blue), Fe (red) and O (green). b) TEM images of crosssectioned area of the nanocomposite.
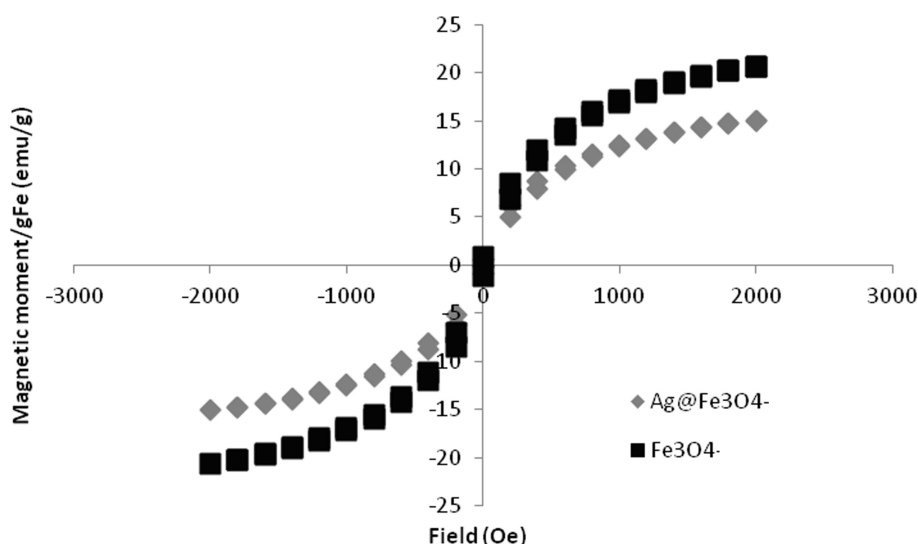

Figure 10. SQUID magnetization curves of Fe$_3$O$_4$- and Ag@Fe$_3$O$_4$- nanocomposites.

Similar magnetic hysteresis curves and saturation values were obtained when comparing both nanocomposites, suggesting that the presence of Ag did not affect the magnetic properties of the material. This was especially relevant when considering the final application of the nanocomposites, for example, for water purification.

It is generally known that Ag-NPs are much more toxic than the bulk Ag metal, limiting their application to real live environments. Thus, the possibility of collecting Ag@Fe$_3$O$_4$-NPs accidentally released from the polymeric matrix with a simple magnetic trap would be extremely desirable for water purification. Further studies about the use of Ag-based nanocomposites (and containing a magnetic core) for water treatment applications is detailed in the next section.

4. Ecological concerns regarding uncontrollable release of NPs to the environment

4.1. Environmental and safety concerns and uncontrollable release of NPs

The use of engineered nanoparticles in the environment as a consequence of the development of nanotechnology is a serious case of concern of environmental biologists worldwide. However, a few studies have already demonstrated the toxic effects of NPs on various organisms, including mammals. Nanotechnology is still in discovery phase in which novel materials are first synthesized in small scale in order to identify new properties and further applications [26–31].

Perception and knowledge are important parts of public understanding of nanotechnology. They can be influential for achievable benefit obtained and the possible risks and hazards.

Therefore, detail understanding of their sources, release interaction with environment, and possible risk assessment would provide a basis for safer use of engineered nNPs with minimal or no hazardous impact on environment. Thus, ecotoxicology of NPs will be closely related to their intrinsic properties as shown in Table 4 and Figure 11.

Physicochemical properties	Toxicological findings	Biological Effects
Size	Affects reactivity and permeability of cells and organs.	Increase biodistribution of NPs in environmental system.
Surface /volume ratio	Higher reactivity	Inflammatory effects
Chemical Composition	Increase in UVA absorption, higher activation of reactive oxygen species in cell media.	Cancerigen, cell proliferation reduced.
Aggregation state	More pronounced cytotoxic effects	Cytotoxicity
Surface Charge	Charged NPs present higher deposition degree in tissues.	Bioacummulation in brain, lungs and others.

Table 4. Biological effects due to physicochemical properties of nanomaterials 27.

Increase surface activity, mobility, and diffusion and adsorption ability are some other effects [26].

A further comprehension of the structure- function relationships in nanomaterials matter could lead to new protocols for nanomaterials manufacture wherein high precision, low waste methods are included [1,32,33].

Some criteria could be taken into account referring to NPs release and effects study:

1. NPs effects should be scale dependent and not the same in larger scale or agglomerates. This means that effects may be quiet different to adopt specific and more appropriate regulations.

2. These differences are based on size, surface chemistry and other specific interactions depending on the scale. Thus, the same material may have different regulations through the different sizes presented.

3. Effects must be conclusive to those products which commercialization is imminent. So, the NPs presented in the final product may be the ones, which the studies should focus on.

4. For the novelty of some materials, data to extrapolate environmental effects are difficult to obtain; so enhanced simulation system are needed.

The wide application of engineered NPs and their entry into the environment, the study of their impact on the ecosystem and a growing concern in society regarding the possible adverse effects of manufactured nanoparticles has been raised in recent years [26–31,34–39].

Therefore, it is required to study their release, uptake, and mode of toxicity in the organisms. Furthermore, to understand the long-term effect of NPs on the ecosystem, substantial information is required regarding their persistence and bioaccumulation.
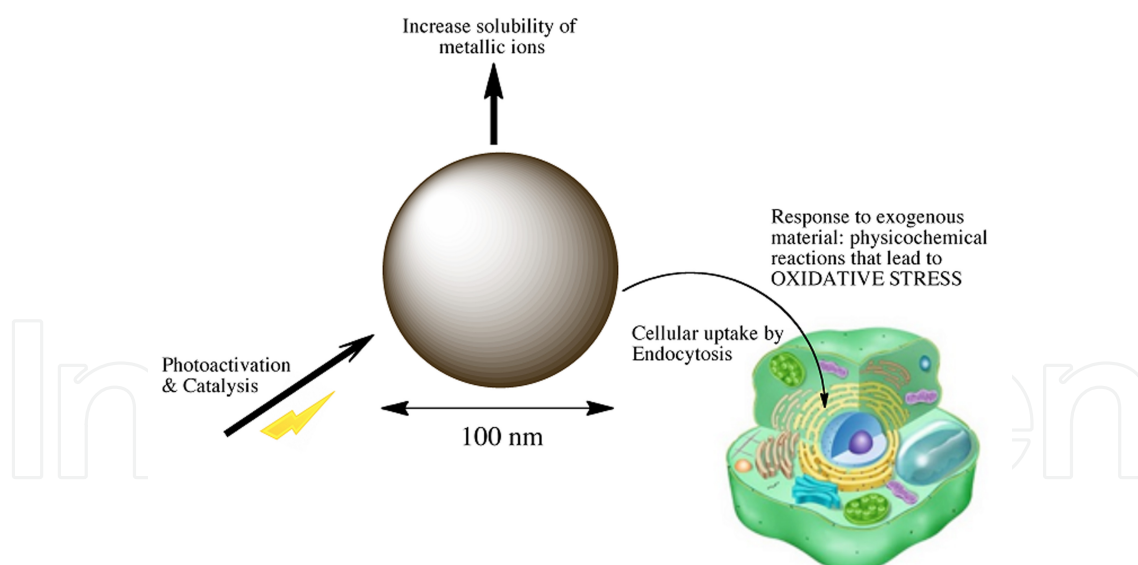

Figure 11. Effects on cellular activity due to the release of metal contain of NPs to the environment.

4.2. Safe polymer-metal nanocomposites

Table 5 presents some of green chemistry principles could be applied to the synthesis of nanomaterials, including nanocomposites.

General Principle	Toxicological findings
Safer nanomaterials	Find the influence of morphology, functionality and other features of nanomaterials that lead to the properties of interest , avoiding and understanding whatever parameter which leads to the incorporation of toxic nature to the material.
Reduced environmental impact	Analyse degradation and routes of incorporation to the environment, looking for a design of harmless products. One possibility is avoid the use of known hazardous precursors for the nanomaterials.
Waste reduction	Optimize solvent use by applying alternative purification techniques and media reactions.
Overall process safety	Make use of benign precursors and solvents in the designing and enhancement of the synthesis and even suggest greener alternative procedures and reagents for existing methodologies.
Materials efficiency	Think about new strategies that incorporate raw materials in products by bottom-up strategy. Also the application of catalytic procedures to enhance selectivity and yield of the overall process.
Energy efficiency	Design room temperature synthetic routes, with real time monitoring to optimize energy consumption.

Table 5. Advisable enhancements for nanomaterial synthesis methodology [1].

The environmental safety of materials, which consist of or contain nanosize components, becomes one of the most important emerging topics of the Nanotechnology within the last few years. The main concerns dealing with the rapid development and commercialization of various nanomaterials are associated with [32,40,41]:

1. the approved higher toxicity of many nanomaterials (NMs) in comparison with their larger counterparts,

2. the absence of the adequate analytical techniques for detection of NMs in the environment

3. the absence of the legislation normative for permitted levels of various NMs in water and air.

In this regard the increase of the safety of NMs is of particular importance. One way to prevent risk is the development of the environmentally-safe polymer-metal nanocomposite materials that consist in a functional polymer with immobilized MNPs distributed mainly by the surface of the polymer with a higher stability to prevent release of the MNPs.

The material represents what makes them maximally accessible for the bacteria to be eliminated. Core-shell MNPs contain a superparamagnetic core coated with the functional metal shell, which provides the maximal bactericide activity. The MNPs are strongly captured in-

side the polymer matrix that prevents their escape into the medium under treatment. The superparamagnetic nature of MNPs provides an additional level of the material safety as MNPs leached from the polymer matrix can be easily captured by the magnetic traps to completely prevent any post-contamination of the treated medium.

4.2.1. Characterization of MNPs: key factor to ensure the safety of new technologies.

Nevertheless, the lack of specific characterization techniques of environmental effects of MNPs, existing and described methodologies should be modified to obtain valid results.

Some parameters must be taken into account in order to understand the relation between NPs behaviour and their physical and chemical structure [1,32,37,41,42].

Without detailed material physicochemical characterization, toxicity studies become difficult to interpret, and inter-comparison of studies becomes near impossible. Factors such as agglomeration state, surface chemistry, material source, preparation method, and storage take on a significance that has often been overlooked, potentially leading to inappropriate conclusions being drawn. Table 6 presents some approaches to the nanotoxicity evaluation [39,42].

This becomes particularly significant where hazard is dependent on structural and surface properties, as changes in these properties may lead to significant differences between the released (or basic) material, and the material people are exposed to. With no specific characterization techniques for nanotoxicity, the actual techniques are being modified and enhanced to determine and evaluate NPs effects.

5. Ecological safe MNPs or MONPs nanocomposites for bactericidal applications for water treatment.

Due to their relevant optical, electrical and thermal properties; Ag-NPs are being incorporated into several commercially available products such as biological and chemical sensors; as well as into bactericidal processes. The antibacterial features of Ag-NPs are one of the top topics of investigation into noble metals research.

Products as wound dressings and biomedical devices with Ag-NPs continuously release Ag in low levels that leads to protection against bacteria.

Considering the unusual properties of nanometric scale materials in contrast with those from macro counterparts, Ag-NPs are widely used for the more efficient antimicrobial activity compared with Ag^+ ions. The incorporation of magnetic cores to the preexisting nanocomposite materials increases the applicability of these in a macro scale for the easiest separation and the enhanced performance [43–47].

5.1. Bactericidal activity test for sulfonated nanocompositescontaining Ag@Co-NPs

In general, the bactericidal activity was determined as the relationship between the number of viable bacteria before and after the treatment in percentage terms (% cell viability) at sev-

eral extractions/treatment times in all the tests Eq. 12)where t_f corresponds to the extraction time and t_o to the initial time).

$$\%CellViability = \frac{\left(CFU\middle/mL\right)_{t_f}}{\left(CFU\middle/mL\right)_{t_0}} \, x \, 100 \tag{12}$$

The relationship between the Ag metal content in the sulfonated polymeric matrix and its antibacterial activity was then evaluated by following both batch and flow protocols.

The capacity of the nanocomposites to inhibit bacterial proliferation was evaluated by using the Minimum Inhibitory Concentration (MIC) test as a batch protocol, by using E. Coli. MIC is definedas the concentration of an antimicrobial agent that completely inhibits the microorganisms' proliferation in the sample. [23] Parallelly, the MIC_{50} corresponds to the antimicrobial concentration which inhibits just the 50%. In this case, the MIC of each material was determined by introducing an increasing amount of nanocomposite (in individual wells, from Microtiter plates with 96 wells,containing 10^5 CFU/mL of E. coli suspension in LB medium. After overnight incubation, bacterial proliferation was evaluated by measuring the optical density of each well at 550 nm (this wavelength is indicative of bacterial proliferation). The bactericidal activity of the Ag, Co and Ag@Co nanocomposites (in sulfonated polymeric granulated matrices) was determined as showin in Figure 12. As a result, the MIC_{50} values are expressed as number of nanocomposite beads in 200 μL of culture medium (beads/200 μL).

Assay / Technique	Aim	NPs applicability.
Synchrotron radiation based techniques	Distribution of NPs in different systems, analyze Oxidative Stress precursors, chemical speciation	Nanoscale zerovalent iron, TiO_2, ZnO, CeO_2. NPs
Colony forming efficiency Test	Cytotoxicity	Cobalt NPs
Transmission electron Microscopy (TEM)	Intracellular location, morphology.	Fullerene derivatives, ultrafine particles, metal NPs as AgNPs
Light Microscopy	Morphological observations	Single – wall carbon nanotubes, metal nanoparticles.
Neutral red Assay	Cell viability	Carbon nanotubes, Ag-NPs, Ti-NPs, TiO_2-NPs

Table 6. Overview of different techniques and assays for nanotoxicity evaluation.

The raw sulfonated material did not present inhibitory activity in the concentration range under test. However, it became antibacterial when modified with NPs providing a quite higher value of MIC_{50} (between 13-16 beads/200 μL) compared with that of Ag@Co- nano-

composites with the same Ag content (MIC$_{50}$ around 4 beads/200 μL). The reason for the enhancement inhibition of bacteria proliferation recorded by Ag@Co-NPs in sulfonated matrices is still controversial. However, thanks to the better knowledge of Ag@Co-granulated nanocomposites obtained by further characterization with different techniques, it is possible to link some physic-chemical parameters with the final bactericidal activity of the materials.This best result is in agreement with the reported value for organo-silver compounds incorporated in microspheres (~ 0.125 mM) [24].
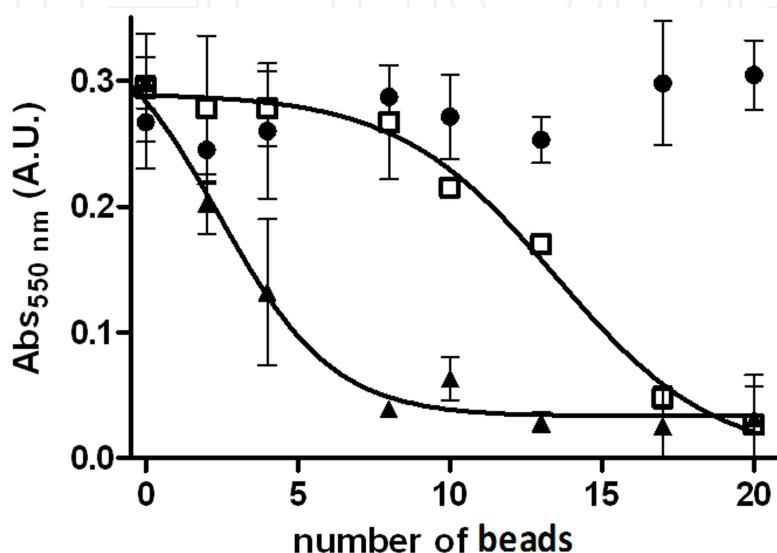

Figure 12. Variation of the absorbance at 550 nm with the number of polymer beads for (●) the raw material, (□) Ag-and, (▲) Ag@Co-sulfonated (C100E) nanocomposites (3 replicates).

In the flow method, nanocomposite-based filters containing Ag@Co-NPs or without NPs were set in a filtering column support of the experimental set-up and connected to a peristaltic pump that allowed the control of the flow rate. This set-up can operate by a single pass, when bacterial suspensions passed through the filter containing nanoparticles only once. The number of viable cells was determined at regular times. 10^3 CFU/mL of E. coli suspensions were forced to pass through the filter at a flow rate of ranging 1.0mL/min and the bactericidal activity of the material was evaluated.

Culture medium samples after passing through the column were extracted once a week under sterile conditions and the number of viable cells was determined. Figure 14 compares the % cell viability versus treatment time for sulfonated granulated material modified with Ag- or Ag@Co-NPs. Also, raw material response is shown.

The cell viability in the suspension after being treated by sulfonated nanocomposites for 60 min of continuous operation was found to decrease near to 0 %. Also, little differences between Ag and Ag@Co stabilized in different polymeric matrices are observed. It should be emphasized that, in this case, control samples showed also a decrease of % cell viability after 60 min of treatment. Therefore, these nanocomposites showed good performance and stability even under continuous operation.
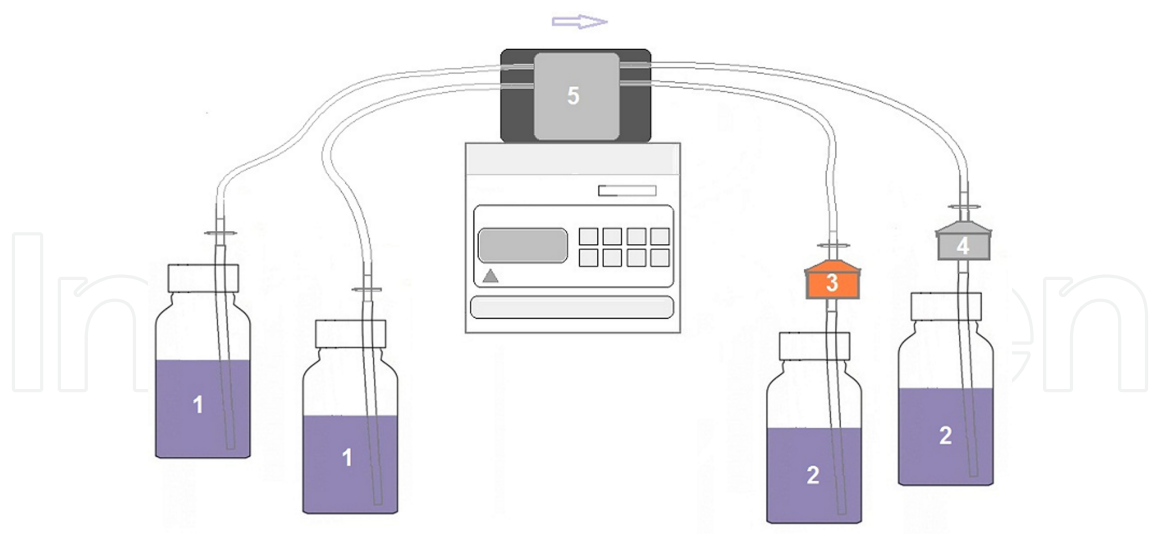
Figure 13. Scheme of the flow experimental one-step where:1. Initial Bacterial suspension, 2. Treated solution, 3. Nanocomposite filter (Ag@Co-NPs), 4. Control filter (without NPs), 5. Pump.

As it aforementioned, the Ag@Co-nanocomposites bactericidal activity was evaluated in granulated polymers. The nanocomposite showed high bactericidal activity with a cell viability close to 0 % for bacterial suspensions with an initial concentration below 10^5 CFU/mL) and only the more concentrated suspensions (over 10^5 CFU/mL) required recirculation to guarantee a complete bacterial removal.
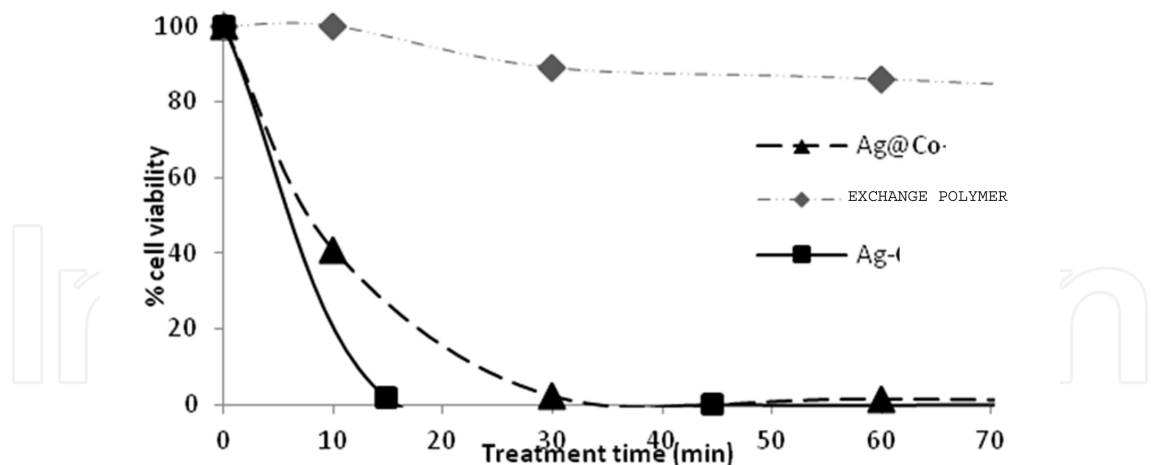

Figure 14. Representation of the variation of the % of cell viability with the treatment time for the Ag-, Ag@Co- and raw sulfonated granulated nanocomposite.

Also, the materials lifetime was tested obtaining high activities for different kinds of bacteria and applied in long term experiments. It was observed in all cases that bimetallic Ag@Co-NPs in any type of support showed higher bactericidal activity in comparison with monometallic Ag- or Co-NPs. However, the presence of Co showed high toxicity [14].

5.3. Bacterial applications test for solfonated granulated resins containing Ag@Fe$_3$O$_4$ nanocomposites.

Hence, the described Ag@Fe$_3$O$_4$-nanocomposites were tested and compared for antibacterial applications. In general, their antibacterial activity was evaluated by quantifying cell viability (% cell viability) at several extractions/treatment times after incubation with the E.coli bacteria by following the batch protocol as shown in Figure 15. It is determined the kinetics in terms of % of cell viability per mg of Ag for the samples to compare the activity for Ag- or Ag@Fe$_3$O$_4$-NPs on C100E polymers.
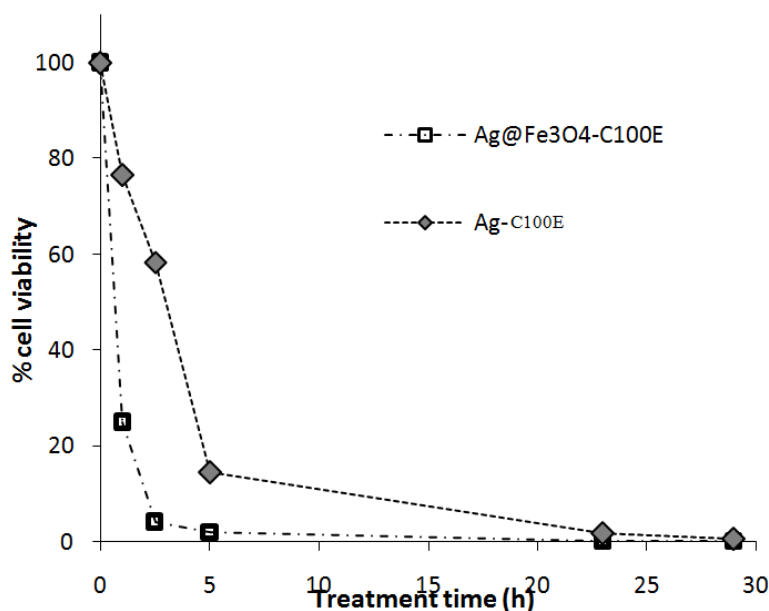

Figure 15. Cell viability versus treatment time for Ag@Fe$_3$O$_4$- nanocomposites in sulfonated polymers.

All the Ag@Fe$_3$O$_4$ samples showed initially, a fast decrease in cell viability what corresponds to a decrease of more than the 90 % after 2.5 h of treatment.

5.4. Bactericidal applications test for ammine based nanocomposite containing Ag@Fe$_3$O$_4$-NPs

The capacity of the nanocomposites to inhibit bacterial proliferation was evaluated by using the MIC test [24] by using E. Coli as described before.

The MIC of both Ag- and Ag@Fe$_3$O$_4$-A520E was determined and compared with that obtained by the raw material without NPs or containing Fe$_3$O$_4$-NPs as shown in Figure 16.

Ag- and Ag@Fe$_3$O$_4$-A520E nanocomposites showed high bactericidal activity with a deep decrease of the absorbance magnitude at 550 nm (Abs$_{550}$ when increasing the number of nanocomposite beads in the suspension. Conversely, raw material and Fe$_3$O$_4$-nanocomposite

did not present significant bactericidal activity at this concentration range, with a constant Abs_{550} value around 0.4 a.u. in all cases.

This result indicated that Ag-NPs were responsible of the bactericidal activity recorded and it was not affected by the presence of magnetite.
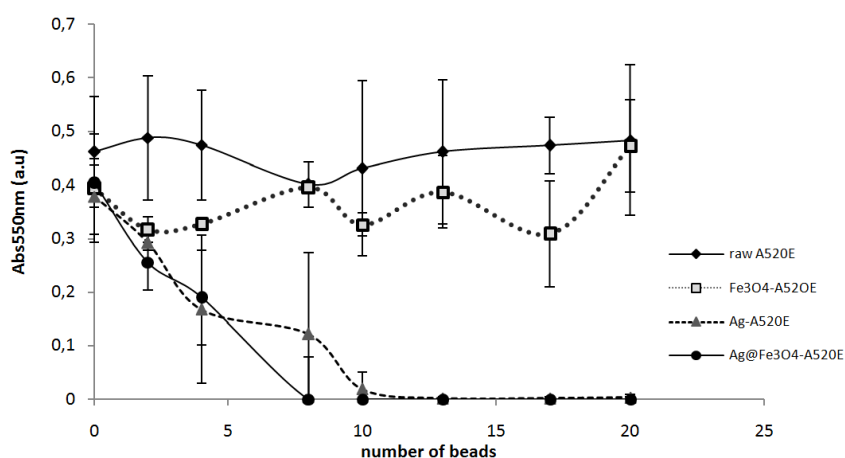

Figure 16. Variation of the absorbance at 550 nm with the number of polymer beads for the Ag- and Fe_3O_4-based A520E nanocomposites. Raw material is also analysed (3 replicates).

6. Conclusions

The following conclusions could be derived from the results and discussion shown in this chapter.

• It was shown that the Intermatrix Synthesis (IMS) method is applicable to all the ion-exchange materials tested and useful to any kind of NPs composition since, also, the coupling of the IMS with the co-precipitation technique was succeed to obtain magnetite-based nanocomposites.

• IMS methodology coupling with Donnan Exclusion Effect was observed for the NPs structures synthesized on the ion exchange polymers. All NPs were highly stabilized on the surface of the polymer and showed magnetic properties what allows their recovery by applying a magnetic trap.

• Also, the development of the IMS route to the synthesis of NPs on anion exchanger polymers was obtained showing comparable results than the materials formed by using catio-nexchangers.

• The rapid growth of interest in engineered NPs has presented many challenges for ecotoxicology, not least being the effort required to analyse and understand the NPs themselves.

- Given the importance of potable water to people, it is a clear need for the development of innovative new technologies and materials whereby challenges associated with the provision of safe potable water can be addressed.

- Ag@Co and Ag@Fe_3O_4-NPs stabilized in both anion and cationexchanger polymeric resins were applied for the water purification against E.coli bacteria suspensions. Both NPs structure showed high bactericidal activity being, however, less citotoxic the materials containing Fe_3O_4-NPs.

- Thus, an efficient material based on Ag@Fe_3O_4-NPs stabilized in anion and cation exchanger polymeric resins was obtained for water treatment applications by showing high bactericide activity as well as low citotoxity for animal cells.

Acknowledgements

Author details

Amanda Alonso[1], Julio Bastos-Arrieta[1], Gemma.L. Davies[2], Yurii.K. Gun'ko[2], Núria Vigués[3], Xavier Muñoz-Berbel[4], Jorge Macanás[5], Jordi Mas[3], Maria Muñoz[1] and Dmitri N. Muraviev[1]

*Address all correspondence to: Dimitri.Muraviev@uab.cat

1 Analytical Chemistry Division, Department of Chemistry, Autonomous University of Barcelona, 08193 Bellaterra, Barcelona, Spain

2 Trinity College Dublin, Dublin 2, , Ireland

3 Department of Genetics and Microbiology, Autonomous University of Barcelona, 08913, Bellaterra, Barcelona, Spain

4 Centre Nacional de Microelectrònica (IMB-CNM, CSIC), 08913, Bellaterra, Barcelona, Spain

5 Department of Chemical Engineering, Universitat Politècnica de Catalunya (UPC), 08222, Terrassa, Spain

References

[1] Dahl, J.A., Maddux, B.L.S., & Hutchison, J.E. (2007). Toward greener nanosynthesis. *Chemical reviews [Internet]*, 107(6), 2228-69, http://www.ncbi.nlm.nih.gov/pubmed/17564480.

[2] Campelo, J. M., Luna, D., Luque, R., Marinas, J. M., & Romero, A. A. (2009). Sustainable preparation of supported metal nanoparticles and their applications in catalysis. *ChemSusChem [Internet]*, 2(1), 18-45, http://www.ncbi.nlm.nih.gov/pubmed/19142903.

[3] Erkey, C. (2009). *The Journal of Supercritical Fluids Preparation of metallic supported nanoparticles and films using supercritical fluid deposition*, 47, 517-22.

[4] Han, B. J., Liu, Y., & Guo, R. (2009). *Reactive Template Method to Synthesize Gold Nanoparticles with Controllable Size and Morphology Supported on Shells of Polymer Hollow Microspheres and Their Application for Aerobic Alcohol Oxidation in Water*, 1112-7.

[5] Han, B. J., Liu, Y., & Guo, R. (2009). *Reactive Template Method to Synthesize Gold Nanoparticles with Controllable Size and Morphology Supported on Shells of Polymer Hollow Microspheres and Their Application for Aerobic Alcohol Oxidation in Water*, 1112-7.

[6] Macanás, J., Bastos-arrieta, J., Shafir, A., Alonso, A., Mu, M., & Muraviev, D.N. (2012). *Article in press*, 10-3.

[7] Muraviev, D. N., Alonso, A., Shafir, A., & Vallribera, A. (2012). *Article in press*.

[8] Muraviev, D., Macanas, J., Farre, M., Munoz, M., & Alegret, S. (2006). Novel routes for inter-matrix synthesis and characterization of polymer stabilized metal nanoparticles for molecular recognition devices. *Sensors and Actuators B: Chemical [Internet]*, *[cited 2011 May 9]*, 118(1-2), 408-17, http://linkinghub.elsevier.com/retrieve/pii/S092540050600325X.

[9] Parrondo, J., & Mun, M. (2007). *Cation-exchange membrane as nanoreactor: Intermatrix synthesis of platinum- copper core- shell nanoparticles.*, 67, 1612-21.

[10] Ruiz, P., Muñoz, M., Macanás, J., & Muraviev, D.N. (2011). Reactive & Functional Polymers Intermatrix synthesis of polymer-stabilized PGM @ Cu core- shell nanoparticles with enhanced electrocatalytic properties. *Reactive and Functional Polymers [Internet]*, 71(8), 916-24, http://dx.doi.org/10.1016/j.reactfunctpolym.2011.05.009.

[11] Taylor, P., Muraviev, D. N., Pividory, M. I., Luis, J., & Soto, M. (2012). *Solvent Extraction and Ion Exchange Extractant Assisted Synthesis of Polymer Stabilized Platinum and Palladium Metal Nanoparticles for Sensor Applications Extractant Assisted Synthesis of Polymer*.

[12] Barbaro, P., & Liguori, F. (2009). Ion exchange resins: catalyst recovery and recycle. *Chemical reviews [Internet]*, 109(2), 515-29, http://www.ncbi.nlm.nih.gov/pubmed/19105606.

[13] Zegorodni, A. (2006). Ion exchange material. *Elsevier [Internet], [cited 2012 May 27]*, http://www.sciencedirect.com/science/book/9780080445526.

[14] Alonso, A., Muñoz-Berbel, X., Vigués, N., Rodríguez-Rodríguez, R., Macanás, J., Mas, J., et al. (2012). Intermatrix synthesis of monometallic and magnetic metal/metal oxide nanoparticles with bactericidal activity on anionic exchange polymers. *RSC Advances [Internet], [cited 2012 Apr 27]*, 2(3), 4596-9, http://xlink.rsc.org/?DOI=c2ra20216.

[15] Kung, H.H., & Kung, M.C. (2004). Nanotechnology: applications and potentials for heterogeneous catalysis. *Catalysis Today [Internet], Nov [cited 2011 Aug 3]*, 97(4), 219-24, http://linkinghub.elsevier.com/retrieve/pii/S0920586104004262.

[16] Alonso, A., Macanás, J., Shafir, A., Muñoz, M., Vallribera, A., Prodius, D., et al. (2010). Donnan-exclusion-driven distribution of catalytic ferromagnetic nanoparticles synthesized in polymeric fibers. *Dalton transactions (Cambridge, England: 2003) [Internet], Mar [cited 2011 Feb 24]*, 39(10), 2579-86, http://www.ncbi.nlm.nih.gov/pubmed/20179851.

[17] Ayyad, O., Muñoz-Rojas, D., Oró-Solé, J., & Gómez-Romero, P. (2009). From silver nanoparticles to nanostructures through matrix chemistry. *Journal of Nanoparticle Research*, 12(1), 337-45.

[18] Lira-Cantú, M., & Gómez-Romero, P. (1997). Cation vs. anion insertion in hybrid materials based on conducting organic polymers for energy storage applications. *Ionics*, 3(3-4), 194-200.

[19] Ruiz, P., Muñoz, M., Macanás, J., Turta, C., Prodius, D., & Muraviev, D. N. (2010). Intermatrix synthesis of polymer stabilized inorganic nanocatalyst with maximum accessibility for reactants. *Dalton transactions (Cambridge, England: 2003) [Internet], Feb [cited 2011 Feb 24]*, 39(7), 1751-7, http://www.ncbi.nlm.nih.gov/pubmed/20449418.

[20] Ruiz, P., Muñoz, M., Macanás, J., & Muraviev, D. N. (2010). Intermatrix Synthesis of Polymer−Copper Nanocomposites with Tunable Parameters by Using Copper Comproportionation Reaction. *Chemistry of Materials [Internet], Dec [cited 2011 Feb 24]*, 22(24), 6616-23, http://pubs.acs.org/doi/abs/10.1021/cm102122c.

[21] Muraviev, D. N., Ruiz, P., Muñoz, M., & Macanás, J. (2008). Novel strategies for preparation and characterization of functional polymer-metal nanocomposites for electrochemical applications. *Pure and Applied Chemistry [Internet], cited 2011 Feb 24]*, 80(11), 2425-37, http://iupac.org/publications/pac/80/11/2425/.

[22] Muraviev, D.N., Macanás, J., Ruiz, P, & Muñoz, M. Synthesis, stability and electrocatalytic activity of polymer-stabilized monometallic Pt and bimetallic Pt/Cu core-shell nanoparticles. *Physica Status Solidi (a) [Internet]. 2008 Jun [cited 2012 May 23]*, 205(6), 1460-4, http://doi.wiley.com/10.1002/pssa.200778132.

[23] Ferreira, T. A. S., Waerenborgh, J. C., Mendonça, M. H. R. M., Nunes, M. R., & Costa, F. M. (2003). *Structural and morphological characterization of FeCo 2 O 4 and CoFe 2 O 4 spinels prepared by a coprecipition method*, 5, 383-92.

[24] Alonso, A. (2012). Development of polymeric nanocomposites with enhanced distribution of catalytically active or bactericide nanoparticles. *PhD Thesis. Universitat Autònoma de Barcelona.*

[25] Poulter, N., Muñoz-Berbel, X., Johnoson, A.L., Dowling, A.J., Waterfield, N., & Jenkis, T.A. (2009). *Chemical Communications*, 7312-7314.

[26] Toksha, B. G., Shirsath, S. E., Patange, S. M., & Jadhav, K. M. (2008). *Structural investigations and magnetic properties of cobalt ferrite nanoparticles prepared by sol- gel auto combustion method*, 147, 479-83.

[27] Search, H., Journals, C., Contact, A., & Iopscience, M. (2003). Address IP. *Applications of magnetic nanoparticles in biomedicine*, 167.

[28] Amara, D., Felner, I., Nowik, I., & Margel, S. (2009). *Colloids and Surfaces A: Physicochemical and Engineering Aspects Synthesis and characterization of Fe and Fe 3 O 4 nanoparticles by thermal decomposition of triiron dodecacarbonyl*, 339, 106-10.

[29] Æ, PCÆFVDK, & Hofmann, MBÆT. (2008). Nanoparticles: structure, properties, preparation and behaviour. *Environmental media*, 326-43.

[30] Arora, S., Rajwade, J. M., & Paknikar, K. M. (2012). Nanotoxicology and in vitro studies: The need of the hour. *Toxicology and Applied Pharmacology [Internet]*, 258(2), 151-65, http://dx.doi.org/10.1016/j.taap.2011.11.010.

[31] Blaser, S. A., Scheringer, M., Macleod, M., & Hungerbühler, K. (2007). Estimation of cumulative aquatic exposure and risk due to silver: Contribution of nano-functionalized plastics and textiles. *Europe*.

[32] Cushen, M., Kerry, J., Morris, M., Cruz-romero, M., & Cummins, E. (2011). Nanotechnologies in the food industry e Recent developments, risks and regulation. *Trends in Food Science & Technology [Internet]*, http://dx.doi.org/10.1016/j.tifs.2011.10.006.

[33] Chen-fang, M., & Li-lan, H. (2007). The consumer' s attitude toward genetically modified foods in Taiwan. *Food Quality and Preference*, 18(40), 662-74.

[34] Innovation, N., & Island, R. (2010). Ion Release Kinetics and Particle Persistence in Aqueous Nano-Silver Colloids. *Environmental Science & Technology*, 2169-75.

[35] Ry, G. V. L. O. W., Rez, P. A. L. V. A., Ysios, D. I. A. N., Ysiou, D., & Biswas, P. R. A. Assessing the Risks of Manufactured. *Environmental Science & Technology*.

[36] Maynard, A.D. (2006). *Nanotechnology: Nanotechnology is seen as a transformative technology, which has the*, 1(2), 22-33.

[37] Wagner, B., Marconi, F., Kaegi, R., Odzak, N., & Box, P. O. (2008). *Toxicity of Silver Nanoparticles to Chlamydomonas reinhardtii*, 8959-64.

[38] Tiede, K., Hassellöv, M., Breitbarth, E., Chaudhry, Q., Boxall, A.B.A., Hutton, S., et al. (2009). *Considerations for environmental fate and ecotoxicity testing to support environmental risk assessments for engineered nanoparticles*, 1216, 503-9.

[39] Simonet, B. M., & Valcárcel, M. (2009). *Monitoring nanoparticles in the environment*, 17-21.

[40] Siegrist, M., Cousin-eve, M., Kastenholz, H., & Wiek, A. (2007). *Public acceptance of nanotechnology foods and food packaging: The influence of affect and trust. Appetite*, 49, 459-66.

[41] Press AIN. (2007). Nanotechnologies: What we do not know. *Technology in Society*, 29, 43-61.

[42] Nowack, B. (2008). *Exposure Modeling of Engineered Nanoparticles in the Environment*, 41(0), 4447-53.

[43] Savolainen, K., Pylkkänen, L., Norppa, H., Falck, G., Lindberg, H., Tuomi, T., et al. (2010). Nanotechnologies, engineered nanomaterials and occupational health and safety- A review. *Safety Science [Internet]*, 48(8), 957-63, http://dx.doi.org/10.1016/j.ssci.2010.03.006.

[44] Midander, K., Cronholm, P., Karlsson, H.L., Elihn, K., Leygraf, C., & Wallinder, I.O. (2009). Surface Characteristics, Copper Release, and Toxicity of Nano- and Micrometer-Sized Copper and Copper (II) Oxide Particles: A Cross-Disciplinary Study. *Small* [3], 389-99.

[45] Siegrist, M., Stampfli, N., Kastenholz, H., & Keller, C. (2008). Perceived risks and perceived benefits of different nanotechnology foods and nanotechnology food packaging. *Appetite*, 51, 283-90.

[46] Hu-song, B. J., Zhong-shu, L., Song-guo, W., & Wan-jun, L. (2008). Synthesis of Hierarchically Structured Metal Oxides and their Application. *Heavy Metal Ion Removal*, 2977-82.

[47] Lv, Y., Liu, H., Wang, Z., Liu, S., Hao, L., Sang, Y., et al. (2009). *Silver nanoparticle-decorated porous ceramic composite for water treatment*, 331, 50-6.

[48] Rajh, T., Chen, L. X., Lukas, K., Liu, T., Thurnauer, M. C., & Tiede, D. M. (2002). *Surface Restructuring of Nanoparticles: An Efficient Route for Ligand-Metal Oxide Crosstalk*, 10543-52.

[49] Theron, J., Walker, J. A., & Cloete, T. E. (2008). *Nanotechnology and Water Treatment: Applications and Emerging Opportunities*, 43-69.

[50] Zhon-shu, BL., Hu-song, J., Liang-pu, H., Cao-min, A., Song-guo, W., & Wan-jun, L. (2006). Self-Assembled 3D Flowerlike Iron Oxide Nanostructures and Their Application. *Water Treatment*, 2426-31.